Analysis of Disease Progress of Citrus Canker in Nurseries in Argentina

T. R. Gottwald, L. W. Timmer, and R. G. McGuire

First author: research plant pathologist, U.S. Department of Agriculture, Agricultural Research Service, Horticultural Research Laboratory, Orlando, FL 32803. Second and third authors: professor and postdoctoral research associate, University of Florida, Citrus Research and Education Center, Lake Alfred 33850.

We wish to thank S. Garran for project supervision; N. Timmer, A. Dow, J. Bittle, C. Hurtado, M. Scheifler, V. Scheifler, and V. Figueredo for data collection and technical assistance; and C. L. Campbell and L. V. Madden for consultation on statistical analysis.

Supported in part by U.S. Department of Agriculture/OICD grant IR-AR-FL-137.

Accepted for publication 16 June 1989 (submitted for electronic processing).

ABSTRACT

Gottwald, T. R., Timmer, L. W., and McGuire, R. G. 1989. Analysis of disease progress of citrus canker in nurseries in Argentina. Phytopathology 79:1276-1283.

Three nursery plots of Duncan grapefruit, Pineapple sweet orange, and Swingle citrumelo rootstock were established in Concordia, Entre Rios, Argentina, to study the temporal increase and spatial spread of citrus bacterial canker from a single focal point. Focal trees of each cultivar were inoculated with *Xanthomonas campestris* pv. *citri*, the causal agent of Asiatic citrus bacterial canker, and planted in the center of each plot. Disease increase over time was measured as either disease severity (proportion of leaves infected per plant) or disease incidence (proportion of plants infected). Exponential, monomolecular, logistic, Gompertz, and Weibull models were tested for appropriateness by nonlinear regression analysis. The Gompertz model was superior for describing increase in disease incidence and disease severity in all three citrus nurseries. The rate of disease increase was greater in the most susceptible host, Duncan grapefruit, than in less susceptible hosts, Pineapple orange or Swingle. Disease spread coincided with rain splash dispersal and a rapid increase in the apparent infection rate after windblown rainstorms. Rate of disease spread was independent of wind direction. Aggregation of diseased plants was observed in all three nurseries throughout the duration of the tests. Aggregation of individuals appeared to be equivalent between and across rows, indicating that splash dispersal of inoculum was not impeded by between-row distances. Secondary foci were established early in the epidemics and soon overcame the effect of the original focus of disease. The slope of linearized disease gradients, $[-\ln(-\ln(y)) = a + b \ln(x)$, where y = disease incidence and x = distance from the focus of infection in meters, fluctuated over time because of disease-induced defoliation of severely infected plants. Defoliation of more severely diseased plants near the focus subsequently resulted in positive disease gradient slopes for the susceptible Duncan grapefruit nursery as disease levels near the focus diminished.

Additional keywords: dispersion, isopath, quantitative epidemiology.

Xanthomonas campestris pv. *citri* causes Asiatic citrus bacterial canker (CBC, "citrus canker") in numerous citrus-producing countries worldwide (3,13–15). The disease causes erumpent lesions with chlorotic halos and water-soaked margins on fruit, foliage, and green wood (3). Fruit spotting reduces marketability, and the presence of the disease severely hampers inter- and intracountry movement of citrus because of regulatory measures to preclude entry of the disease into canker-free areas (15). Severe CBC can reduce crop yield as well as quality. In mature trees with severe infestations, defoliation and dieback of green wood may occur (8). Citrus nursery trees with CBC infections are rendered unmarketable if the disease is detected. Infected nursery trees are the primary source of pathogen dissemination over long distances (3,15).

Recent outbreaks of CBC on the Gulf Coast of Florida and of a bacterial spot disease of citrus caused by *Xanthomonas campestris* pv. *citrumelo* pv. nov. in nurseries has resulted in the eradication of more than 22 million citrus trees and stimulated new research on CBC (6,7,10,22,23).

Dissemination of *X. c. citri* is directly related to wind-driven rain, especially when wind speeds exceed 8 m/sec (8,19,24,27). Bacteria exude from lesions when wetted and splash to nearby plants (21,24). Bacterial concentrations of 10^5–10^6 colony-forming units (cfu)/ml have been collected from rainwater on foliage infected with *X. c. citri*, and bacteria of *X. c. citri* have been detected in rainwater up to 32 m from diseased foliage (13). High wind speeds during rain can cause water soaking and can facilitate entry of bacteria through stomatal openings into leaves. Lesion development occurs 7–10 days later (18).

In a previous study, rates of CBC disease increase (k) in infested, mature groves in Argentina, where nonpoint inoculum sources were widespread, were calculated from linearized, Gompertz-transformed data to be 0.04–0.06, 0.1, 0.18, and 0.13–0.24/day from mandarin, satsuma, navel, and sweet orange, respectively (1,3,4). In a recent study, rates of CBC increase were determined from discrete foci of infection in new grove plantings to be 0.005 and 0.009/day for orange and grapefruit, respectively (8). Spread of the disease was directional with the highest rates predominantly to the northeast in response to dissemination by wind-driven rain. Rates of disease increase are affected by scion-rootstock combinations (17).

Disease gradients of CBC in infested groves have been described previously. Slopes of Gompit (y) versus $\log_{10}$ (x) linearized disease gradients, where y = disease incidence and x = distance in meters, ranged from −0.21 to −4.13; however, discrete initial foci of inoculum were not determined (4). In a recent study in which foci were determined, slopes of similarly transformed disease gradients varied over time from −0.713 to −1.237 and +0.048 to −1.856 in orange and grapefruit new groves, respectively (8). This variation was the result of disease-induced defoliation and subsequent infection of regrowth in heavily infected trees near the foci. Disease gradients were flattest in the northwest (downwind) direction. Aggregation of diseased trees occurred throughout the epidemic and was somewhat higher during the earlier stages of the epidemic (8).

Although some information is available on the epidemiology of CBC in orchards and new plantings, the spatial and temporal dynamics of citrus canker in citrus nurseries have not been described previously. Study of the epidemiology of CBC in citrus nurseries is important because movement of infected planting stock is the major means of long-distance disease dissemination. The potential of the disease in and from citrus nurseries is of

concern both in the United States and abroad because of potential plant quarantines, embargoes, and loss of markets. The purpose of this study was to quantitate the spatial and temporal progress of CBC in nurseries from a known focal source on citrus species of different susceptibility.

MATERIALS AND METHODS

Nursery plots of Pineapple sweet orange (*Citrus sinensis* (L.) Osb.), Duncan grapefruit (*C. paradisi* Macfad.), and Swingle citrumelo (*Poncirus trifoliata* (L.) Raf. × *C. paradisi*) were established at the Instituto Nacional de Technologia Agropecuaria, an agricultural experiment station near Concordia, Entre Rios, Argentina, to evaluate the disease dynamics of CBC under field conditions. All plots were planted in rows 0.75 m apart with 15 cm between plants within rows, a common nursery spacing. Plots of oranges and grapefruit were planted with 13 rows and 45 plants per row in January 1986. The Swingle citrumelo plot was established in December 1986 with 15 rows and 67 plants per row. Plots were irrigated by overhead sprinkler about twice per week for 30 min.

Inoculation of focal plants. A strain of *X. c. citri* originally isolated from infected grapefruit leaves was grown on nutrient agar amended with kasugamycin (.016 g/L), cephalhexin (.035 g/L), and daconil (.0125 g/L) at 25 C. Inoculum was prepared by suspending 48-hr-old colonies in sterile distilled water and adjusting the concentration turbidimetrically to approximately 10^8 cfu/ml. The inoculum was atomized onto the foliage of Pineapple orange, Duncan grapefruit, and Swingle seedling trees until runoff. Inoculated plants were enclosed in plastic bags to maintain free moisture and high humidity for approximately 48 hr and placed in a growth chamber at 25 C. Bags were removed, and symptoms were allowed to develop for 15–30 days in a growth room before the plants were planted in the field nurseries. One inoculated plant was planted in the center of the center row of each plot to act as a point focus of disease within the plot.

Sampling design and analysis of temporal disease progression. Disease was assessed visually on every tree in each plot on every sample day. Assessments were made in intervals of 14 to 21 days during the growing season and 30 to 45 days during the winter. Disease progress was followed for 382, 383, and 468 days in the grapefruit, orange, and Swingle plots, respectively. Disease was recorded both as disease severity (number of diseased leaves per total number of leaves per plant) and disease incidence (proportion of trees expressing disease in the nursery as a whole). Disease progression models were tested on each plot as a whole over time and in four quadrants (northeast, southeast, southwest, and northwest) within each plot. The common corner of the quadrants was the central focal plant. The appropriateness of the nonlinear forms of the exponential, monomolecular, logistic, Gompertz, and Weibull models was examined for disease severity and disease incidence data for each nursery by nonlinear regression analysis (2,16,20,26,28). The appropriateness of each model was assessed by examining standard residual plots and tested by correlation analysis of observed versus predicted values. Models with the highest coefficient of correlation were chosen as superior. Rate parameters of the Gompertz model (k) (shown later to be most appropriate) of disease progression of individual directional quadrants within each nursery and (k) between nurseries were compared using t-test for all quadrant combinations.

Analysis of spatial disease progression. Aggregation of diseased plants was determined by ordinary runs analysis for each sampling date within and across rows (17). Aggregation was assessed as the proportion of rows and across-row nursery segments with significant ($P = 0.05$) clustering. Aggregation of diseased plants also was examined using Lloyd's index of patchiness (LIP) (27). All three nurseries were planted in a rectangular lattice. Therefore, each nursery was divided into quadrats consisting of five plants down a row. This quadrat size was chosen because the space occupied by five plants down the row was equivalent to the distance between rows. This quadrat size thus squared the rectangular lattice of plants.

Aggregation of diseased plants also was examined by the use of disease isopath maps. Maps were generated for each nursery for dates corresponding to times early in the development of the epidemic, just after the epidemic had entered a rapid disease increase stage, and at the termination of the epidemic, that is, the last day that data were collected. Contour lines were generated corresponding to 0.05 increments of disease severity. To visualize disease severity, three-dimensional response surface maps were generated for the same data as isopath maps. These were examined to determine the intensity of disease in secondary foci and else-

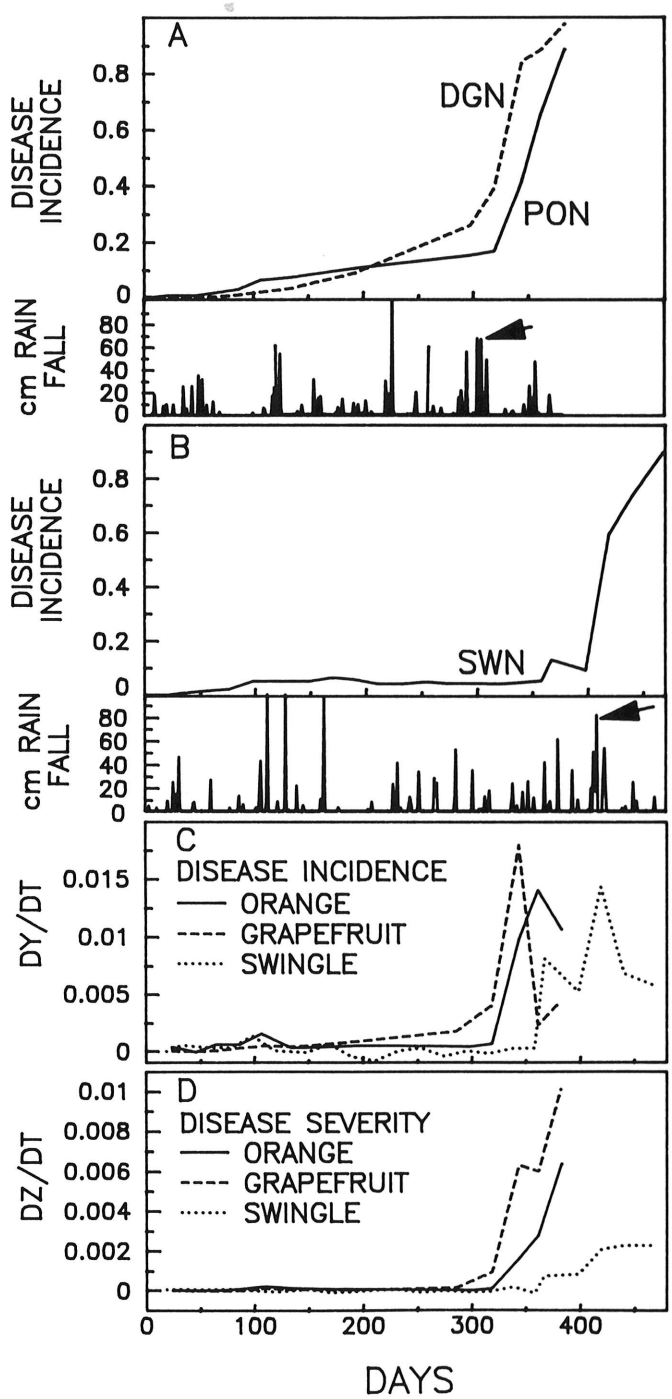

Fig. 1. A and B, Disease incidence of citrus canker over time compared with rainfall. **C and D,** Change in the rate of disease incidence and disease severity, respectively. DGN = Duncan grapefruit nursery; PON = Pineapple orange nursery; SWN = Swingle rootstock nursery. Arrows indicate rainstorms associated with wind in excess of 8 m/sec. DY/DT = the change in disease incidence over time. DZ/DT = the change in disease severity over time.

where within each plot, in relationship to the focus of disease. In addition, they were examined to better understand the directionality of disease spread within and across rows and spatially within the matrix of the nursery plots.

Disease gradient analysis was accomplished by subjecting the spatial arrangement of disease severity assessments to analysis using the GRADCALC program (9). The program calculates the distance from the central focal plant to every other plant in the spatial matrix of the nursery. It then was used to examine weighted means of disease severity, that is, average disease severity divided by the total number of plants falling within 0.5-m-wide concentric bands around the focus. The output data of disease severity versus distance by sampling date was used to generate response surfaces directly. Disease gradients were further analyzed by linear regression of Gompertz-transformed disease regressed on the natural logarithm of the distance from the focal tree.

RESULTS

Analysis of temporal disease progress. Initially disease incidence increased slowly in the three nurseries. Disease occurrence on plants beyond the focal plant was first detected 18, 46, and 46 days after placement in the field for Swingle, grapefruit, and orange nurseries, respectively. In all three nurseries, the proportion of diseased plants remained low for a long period of approximately 300–320 days for grapefruit and orange nurseries and approximately 400 days for the Swingle nursery (Fig. 1). Rain alone did not appear to have an effect on disease increase. However, the absolute rate of disease increase rose noticeably a few days after blowing rainstorms with high winds (indicated by arrows in Fig. 1A and B). Of the nonflexible models evaluated (exponential, monomolecular, Gompertz, and logistic), the Gompertz model was judged to be the most appropriate for describing disease progression (either as disease incidence or disease severity) in all three nurseries based on residual plot analysis and correlation of observed versus predicted values. However, the exponential and logistic models also gave acceptable fits of disease progress data over time (Table 1). In the case of the grapefruit nursery plot, the Gompertz, exponential, and logistic models were nearly equally appropriate in describing the increase of disease proportion over time. Disease severity more accurately reflected the dynamics of disease progression in the field than did disease incidence measurements. Disease-induced defoliation lowered the disease severity on individual plants, whereas disease incidence (+/− disease) remained unchanged. Disease incidence also reached an asymptote in all three nurseries toward the end of the epidemics, whereas no asymptote was reached when disease was measured as disease severity (Fig. 1C and D).

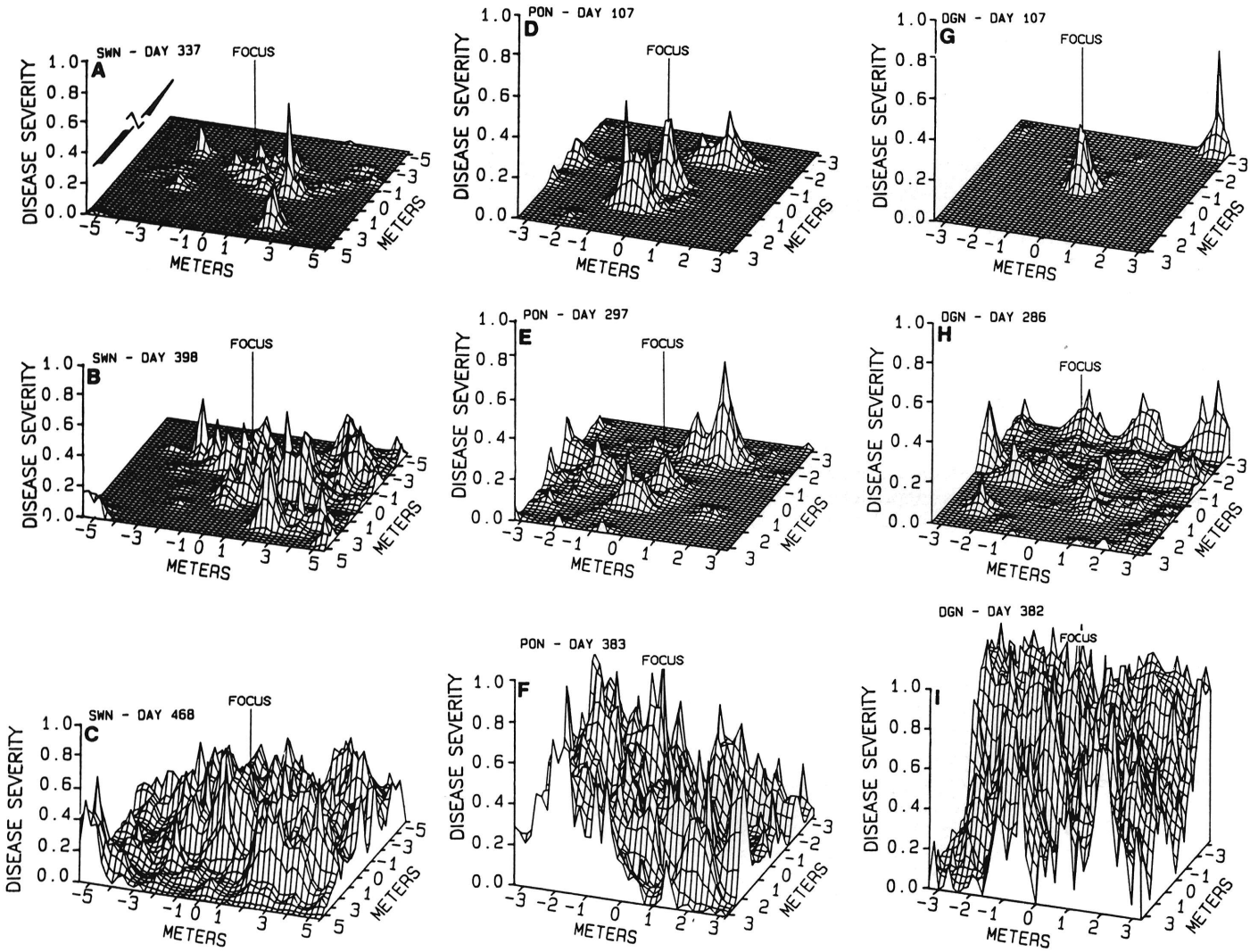

Fig. 2. Three-dimensional response surface representations of citrus canker disease development and spread in three citrus nurseries on the indicated days postinoculation. Note disease incidence of focus (peak) compared to height of peaks of secondary foci. DGN = Duncan grapefruit nursery; PON = Pineapple orange nursery; SWN = Swingle rootstock nursery.

The Weibull model with the location parameter (a) fixed at 1 gave the best overall fit to disease progress data among all models and all plots tested. Coefficients of determination (R^2) of observed versus predicted values ranged from 0.991 to 0.998 (Table 1). However, even when b and c parameters were restricted to small-range estimates, the full Weibull model with a not fixed would not consistently converge. Because the long lag period of low disease intensity at the beginning of the epidemic may have adversely affected the Weibull model performance, one or more of the data points corresponding to the beginning of the epidemic were eliminated. However, the Weibull model still did not converge. Parameter b, the scale parameter, was inversely related to the rate of disease increase. The b parameters were all high, ranging from 331 to 544 days, indicating a slow rate of disease progress of CBC in nurseries compared to other disease situations previously described (20). Parameter c, the shape parameter, was an indication of the inflection point of the rate of disease increase and normally ranges from 1.8 to 9.2 for most disease situations (20,26). Parameter c ranged from 9.89 to 15.09 and indicated that an inflection point of the disease progress curve occurred relatively late in the epidemic.

Because of the lack of convergence by the full Weibull model, the Gompertz model was generally accepted as the preferable model to describe CBC disease increase over time. However, it was recognized that the exponential and logistic models also were appropriate to describe CBC disease increase in most cases.

Gompertz rate parameters (k) for disease incidence and disease severity for all three nurseries are given in Table 1. Rates of disease increase between nurseries were compared via the t-test (Table 2). The rate of disease increase in the Swingle compared to orange nurseries was not significantly different; however, all other combinations of comparisons between nurseries demonstrated significantly different rates of disease increase. Citrus canker progressed slowest in the Swingle nursery and fastest in the grapefruit nursery, although these epidemics were not concurrent.

The Gompertz rate of disease increase also was examined in quadrants within each nursery plot. There were no statistical differences in k among the quadrants within each of the three nurseries except in a single case (Table 3). Here the northeast

TABLE 2. Comparison of slopes from Gompertz model with t-tests for disease incidence and disease severity between nurseries[a] infected with citrus canker

	Disease incidence[b]		Disease severity[b]	
Plot	DGN	PON	DGN	PON
PON	2.394*[c]		2.987**	
SWN	3.449**	1.089	3.839**	0.674

[a]Duncan grapefruit nursery (DGN) vs. Pineapple sweet orange (PON), DGN vs. Swingle citrumelo nursery (SWN), and PON vs. SWN had 22, 32, and 32 degrees of freedom, respectively.
[b]Disease incidence = proportion of diseased plants; disease severity = number of diseased leaves per total number of leaves per plant
[c]*, ** = Significantly different at $P = 0.05$ and $P = 0.01$, respectively. Ho: $b_1 = b_2$, Ha: $b_1 \neq b_2$ where b_n is the slope value of the Gompertz model.

TABLE 3. Comparison of slopes from Gompertz model with t-tests for disease incidence and disease severity between quadrants within nurseries[a] infected with citrus canker

		Disease incidence[c]			Disease severity[c]		
Nursery	Quadrant[b]	NE	SE	SW	NE	SE	SW
DGN	SE	2.066			1.337		
	SW	2.747*[d]	0.836		1.766	0.360	
	NW	0.586	1.355	2.018	0.239	1.410	1.775
PON	SE	0.385			0.222		
	SW	1.477	1.658		1.959	1.837	
	NW	1.146	1.403	0.662	1.412	1.407	0.221
SWN	SE	0.879			0.250		
	SW	1.460	0.798		0.983	1.454	
	NW	1.516	0.853	0.006	1.027	1.514	0.040

[a]Duncan grapefruit nursery (DGN), Pineapple sweet orange nursery (PON), and Swingle citrumelo nursery (SWN) had 22, 22, and 42 degrees of freedom, respectively.
[b]SE = southeast quadrant, SW = southwest quadrant, and NW = northwest quadrant.
[c]Disease incidence = proportion of diseased plants; disease severity = number of diseased leaves per total number of leaves per plant.
[d]* = Significantly different at $P = 0.05$. Ho: $b_1 = b_2$, Ha: $b_1 \neq b_2$ where b_n is the slope value of the Gompertz model.

TABLE 1. Nonlinear regression analysis of disease incidence and disease severity of citrus canker in citrus nursery plantings in Argentina over time

			Disease incidence					Disease severity				
					Asymptotic 95% confidence interval		R^2 of correlation of observed vs. predicted			Asymptotic 95% confidence interval		R^b of correlation of observed vs. predicted
Model[a]	Nursery	Parameter	Estimate	Asymptotic standard error	Lower	Higher	values[b]	Estimate	Asymptotic standard error	Lower	Higher	values[b]
E	Orange	r	0.01579	0.00014	0.01550	0.01609	0.978	0.01120	0.00040	0.01032	0.01210	0.857
E	Grapefruit	r	0.01661	0.00015	0.01628	0.01693	0.974	0.01470	0.00022	0.01421	0.01518	0.956
E	Swingle	r	0.01466	0.00011	0.01444	0.01488	0.968	0.00904	0.00025	0.00852	0.00956	0.888
M	Orange	r	0.00180	0.00044	0.00083	0.00276	0.790	0.00117	0.00039	0.00033	0.00201	0.650
M	Grapefruit	r	0.00242	0.00061	0.00110	0.00374	0.854	0.00137	0.00046	0.00036	0.00238	0.725
M	Swingle	r	0.00097	0.00024	0.00047	0.00146	0.651	0.00072	0.00020	0.00030	0.00114	0.584
L	Orange	r	0.01787	0.00060	0.01657	0.01917	0.9252	0.01148	0.00050	0.01039	0.01257	0.840
L	Grapefruit	r	0.02047	0.00063	0.01910	0.02184	0.970	0.01561	0.00044	0.01464	0.01657	0.924
L	Swingle	r	0.01636	0.00041	0.01551	0.01721	0.922	0.01092	0.00025	0.01040	0.01143	0.903
G	Orange	k	0.02922	0.00477	0.01874	0.03971	0.980	0.01892	0.00143	0.01578	0.02206	0.996
G	Grapefruit	k	0.03179	0.00520	0.02021	0.04338	0.987	0.2343	0.00099	0.02125	0.02561	0.998
G	Swingle	k	0.02860	0.00278	0.02282	0.03437	0.994	0.00956	0.00043	0.00867	0.01044	0.996
W	Orange	b	359.27	2.74	353.24	365.30	0.991	415.88	2.85	409.61	422.14	0.997
		c	12.23	1.57	8.78	15.68		15.09	0.97	12.96	17.21	
W	Grapefruit	b	331.10	2.95	324.62	337.59	0.993	390.07	1.19	387.45	392.70	0.998
		c	10.04	1.31	7.16	12.92		12.19	0.50	11.09	13.30	
W	Swingle	b	428.05	2.55	422.75	433.34	0.992	543.61	6.19	530.75	556.48	0.991
		c	12.27	1.10	9.99	14.45		9.89	0.58	8.68	11.10	

[a]Model parameters were estimated by nonlinear regression of the integrated equations $y = y_0 e^{rt}$, $y = 1 - (1 - y_0)e^{rt}$, $y = 1/[1 + \exp.^{-(\ln(y_0/(1-y_0)) + rt]}$, $y = \exp^{-Be-kt}$, and $y = 1 - \exp^{-((t-a)/b)^c}$ for the exponential (E), monomolecular (M), logistic (L), Gompertz (G), and Weibull (W) models, respectively, where r and k are rate parameters, y is disease measured as incidence or severity, and t is time in days. For the Gompertz model, $B = -\ln(y_0)$. For the Weibull model, a was fixed at 1 to estimate b and c parameters because the model does not converge with all three parameters when they are undefined.
[b]Coefficients of determination of predicted values against observed values to examine appropriateness of models.

quadrant of the grapefruit nursery had a significantly higher k compared with the southwest quadrant of the same nursery.

Analysis of spatial disease progress and aggregation. The three-dimensional response surfaces of disease incidence showed that secondary foci developed soon after disease spread was detected in each nursery (Fig. 2A, D, and G). Peaks of disease incidence of these secondary foci equal to or exceeding that of the focal plant occurred simultaneously with disease spread (Fig. 2A, D, and G). The dominance of the focus was lost early in the epidemic compared with developing secondary foci (Fig. 2B, C, E, F, H, and I). Based on analysis of isopath maps of disease severity, dispersion of inoculum emanating from the focus appeared to be nondirectional and secondary foci coalesced as the epidemic progressed through time (Fig. 3).

Infected plants were highly aggregated throughout the epidemics in all three nurseries, as determined by the significant departure from randomness in an ordinary runs analysis (Fig. 4A and B). In general, aggregation increased in all three nurseries

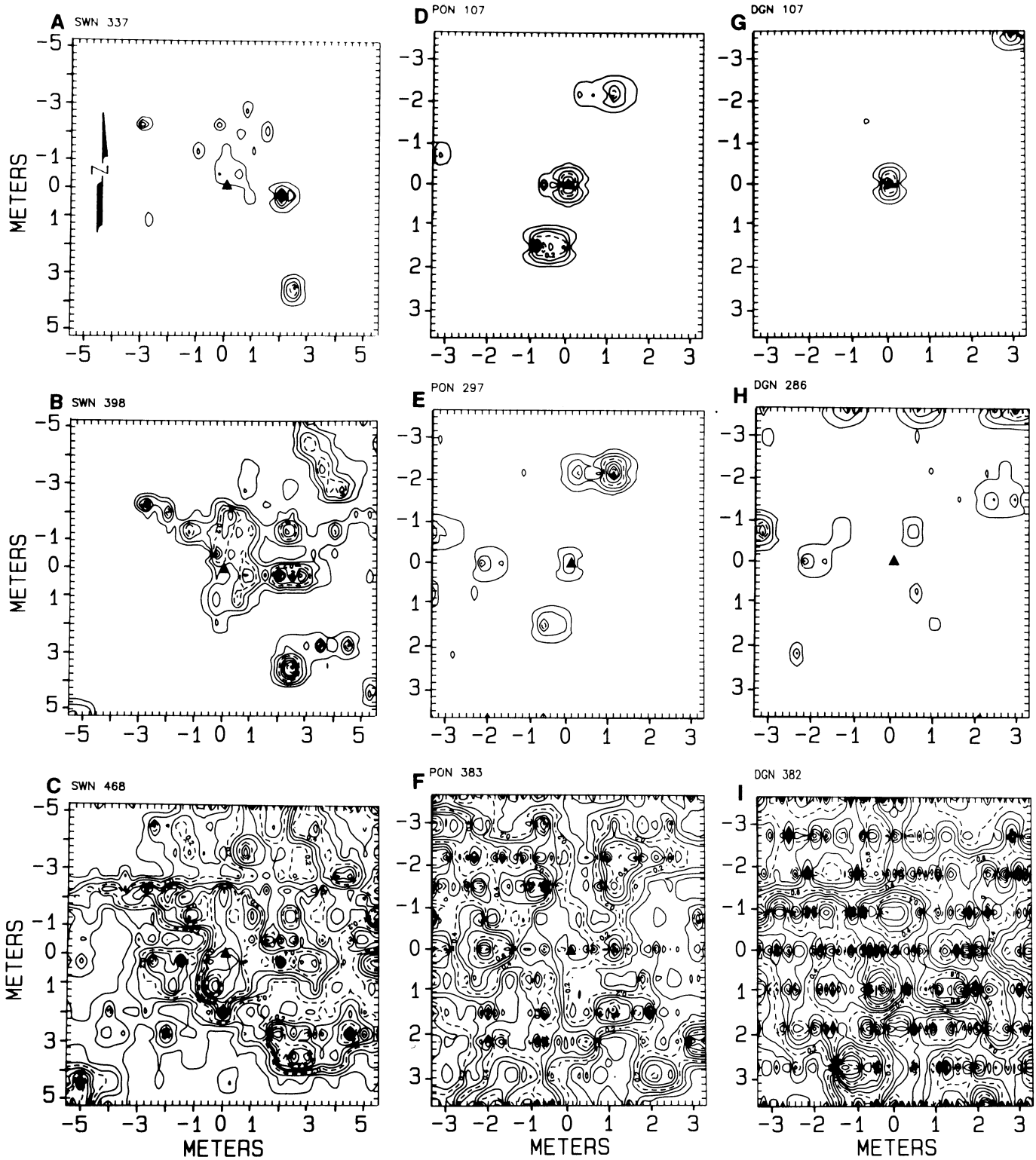

Fig. 3. Isopathic contour maps of citrus canker disease severity on the indicated days postinoculation. Note pattern of dissemination, especially in A, associated with splash dispersal of inoculum, establishment of secondary foci, and eventual coalescence of foci. DGN = Duncan grapefruit nursery; PON = Pineapple orange nursery; SWN = Swingle rootstock nursery. The focal plant is indicated by a triangle, and every fourth line (i.e., disease incidences 0.2, 0.4, 0.6, 0.8, 1.0) is dashed.

over time. The proportion of aggregation across rows often exceeded that within rows. However, the proportion of aggregation within rows exceeded that between rows in the grapefruit nursery plot on the final day (Fig. 4B). This within-row aggregation for the grapefruit nursery is illustrated in the last isopath map which represent a point in time near the end of the study, and which compare the within-row aggregation for the grapefruit nursery (day 382) with those for the Swingle (day 468) and orange (day 383) nurseries (Fig. 3C, F, and I). Similarly, within-row aggregation exceeded across-row aggregation during the first third of the epidemic (day 160) in the orange nursery (Fig. 4B). This also can be seen in the isopath map for the orange nursery (day 107) (Fig. 3D).

In contrast to the aggregation suggested by ordinary runs analysis, LIP decreased over time after an initial increase for all three nurseries, although the analysis suggested aggregation (LIP $>$ 1.0) throughout the duration of all three epidemics (Fig. 4C). Patchiness decreased dramatically in all three nurseries at approximately the same time as pathogen dispersal and disease spread from the inoculated focus were first detected.

Analysis of disease gradients. The use of alternatives to the Gregory model for disease gradients has been proposed. Often the same transformation used in the temporal model of choice also has been used to describe the associated disease gradients (2,4,5,8,10,11). Because the Gompertz model was deemed the most appropriate to describe the temporal disease increase of CBC in citrus nurseries, the model, $-\ln(-\ln(y)) = a + b \ln(x)$ similar to one previously described (4), was used to describe CBC disease gradients, where y = disease incidence and x = distance from the focus of infection (Fig. 4D).

Nontransformed data from the GRADCALC program described above were plotted by date to examine the gradient shapes before linearizing the data (Fig. 5). Disease severity fluctuated at and near the focus over time. The disease severity of plants, within the distances of 0–0.5 and 0.5–1.0 m from the focus, decreased twice during the duration of the epidemic in all three nurseries (denoted by arrows in Fig. 5). The effect of this decrease was the lowering of the slope of the linearized gradients (Fig. 4D). Thus, the slopes did not merely flatten over time as expected but fluctuated over time.

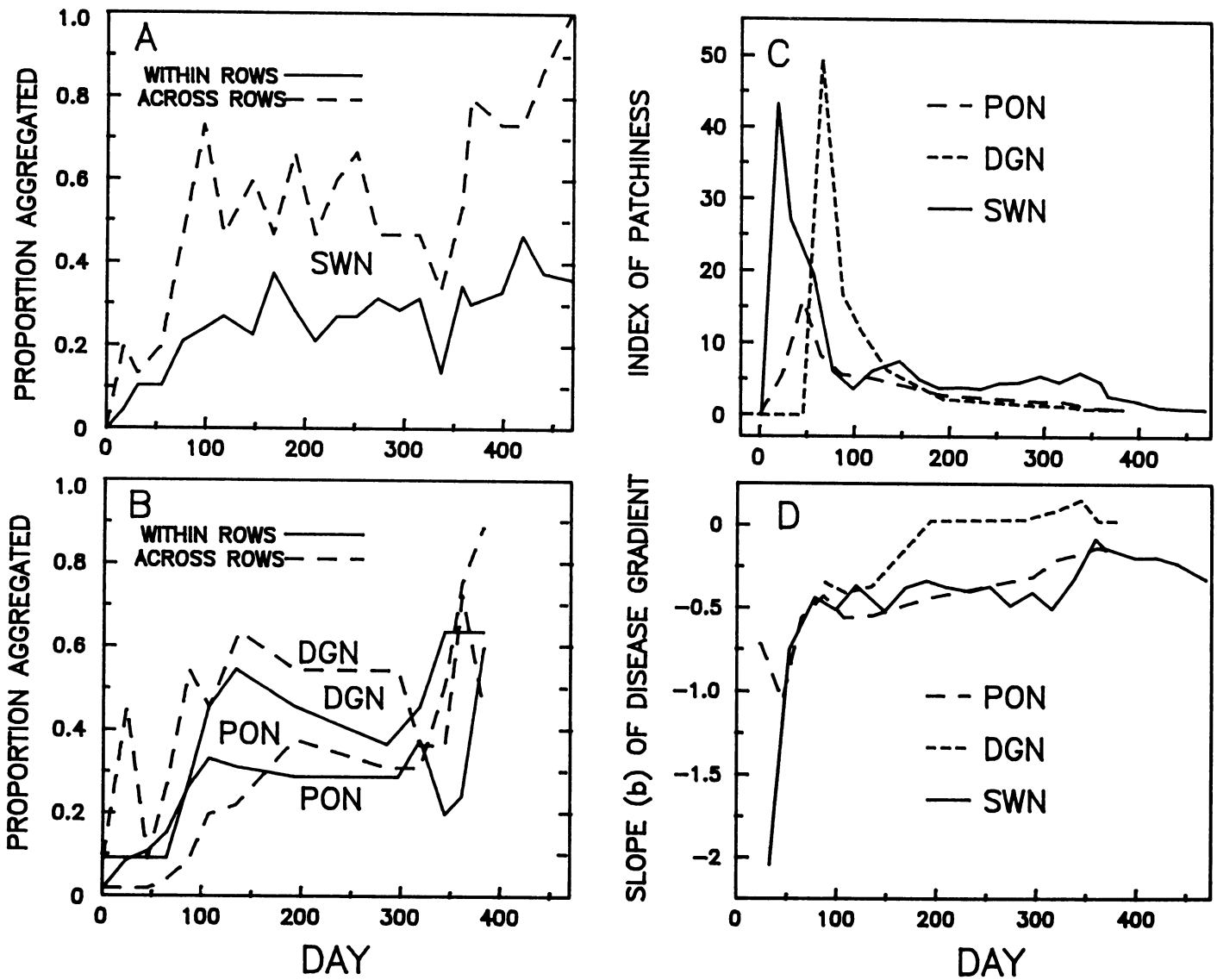

Fig. 4. A and B, Proportion of aggregation of citrus canker-diseased plants over time resulting from ordinary runs analysis. Note that greater aggregation appears to predominate across rows. **C,** Lloyd's index of patchiness expressed over time. **D,** Slopes of disease gradients of three nurseries infected with citrus canker over time. Slopes were generated by regressing $-\ln(-\ln(y)) = a + b \ln(x)$, where y = disease severity, x = distance from the focus in meters, and b = slope of the gradient. Note fluctuations in gradients associated with disease-induced defoliation including positive slope for Duncan grapefruit nursery in later stages of epidemic development. DGN = Duncan grapefruit nursery; PON = Pineapple orange nursery; SWN = Swingle rootstock nursery.

DISCUSSION

Citrus canker disease increase was slow initially in all three nurseries studied. Although minimal disease spread was seen very early in all three epidemics, rains during this period generally were not associated with high wind speeds and temperatures were low for long periods. The abrupt upward inflection in the rate of disease increase immediately following day 319 for grapefruit and orange nurseries and day 398 for the Swingle nursery was directly related to rainstorm events associated with high winds. The association of windblown rain with the spread of CBC has been noted previously (8,24,25). We feel that disease severity as estimated in this study provided more information than disease incidence. Citrus nursery plants, once infected, often caused some of their foliage with symptoms to abscise. The result was that disease severity decreased in those plants while disease incidence remained the same. This decrease in severity was observed in all three nurseries (Fig. 5). Thus, disease severity better reflected the natural fluctuation of CBC within nurseries. In addition, disease progress curves of disease severity never reached asymptotes during the duration of the observed epidemics whereas disease progress curves of disease incidence did (Fig. 1C and D). The lack of asymptotes associated with disease severity better reflects the continuing increase in disease during the time citrus plants normally remain in nursery situations.

The Gompertz model was superior for describing both disease severity and disease incidence over time. As described above, the full (three-parameter) Weibull model did not converge consistently for all three nurseries in this case (27). Disease did not appear to approach an asymptote during the period of time the nursery plots were studied. The duration of the studies was equivalent to or exceeded the duration that citrus plants are normally allowed to remain in a nursery. Under nursery situations, citrus plants flushed and grew almost continuously and new susceptible tissues were added continuously to the pathosystem. Thus susceptible tissue never became limiting. The monomolecular, logistic, Gompertz, and Weibull models all take into account that susceptible tissue becomes limiting as the epidemic progresses. The exponential model, however, does not deal with limited susceptible tissue. Therefore, the simplest model, the exponential, also described CBC adequately in nurseries. The exponential model actually was more appropriate than the Gompertz model when disease values were transformed and the model was fitted by linear regression analysis (Gottwald, *unpublished data*).

The effect of meteorological events was not taken into account in the development of temporal models, yet the influence of blowing rainstorms on disease increase was apparent. Thus, acceptance of the appropriateness of any of the models suggested here should be viewed as preliminary until enough data can be collected to allow the development of more sophisticated temporal models that take into account host growth and major meteorological events.

Gompertz rates of disease increase were significantly different between grapefruit versus Swingle and grapefruit versus orange, but not between Swingle versus orange nurseries (Table 2). These results were consistent with previously reported susceptibility of these cultivars to CBC (1,6,8,19). Grapefruit has long been recognized as one of the most highly susceptible citrus species.

Rates of disease increase generally were not dependent on direction (Table 3). Previous studies in new grove situations indicated a direct association between disease spread in space and disease increase in time with wind direction as the result of severe rainstorms (8). The apparent lack of effect of windblown rain on directionality of spread reported here, except possibly for the grapefruit nursery, and resulting rate of disease increase can best be explained by the geometry of citrus nurseries versus that of citrus groves. In grove situations, trees are normally planted 4–6 m apart in a square or rectangular lattice pattern. Grove trees are also at least 1 m tall. Raindrops hitting a lesion oozing bacteria of *X. c. citri* would, of course, fragment into smaller droplets. Such droplets containing inoculum usually would not reach even the closest neighboring tree in the lattice because of the distance between individuals. However, during rainstorms with high winds, these small droplets would be carried predominantly downwind to neighboring trees (8). Infected grove trees one or more meters tall also raise the origin of inoculum above the boundary layer of air close to the ground and into the turbulent air layers where dissemination and diffusion of inoculum due to eddies are possible. Nursery trees, especially when young, are usually only a few centimeters tall and thus can be affected to some degree by the stagnant boundary air layer. This boundary effect is intensified by the sheltering of numerous other individuals in close proximity. Splash dispersal of inoculum to nearby individuals is much more probable because of the close nursery lattice spacing. Rains without wind are much more common in east central Argentina and, although not as efficient at causing infection, are quite likely to disperse inoculum to nearby individuals

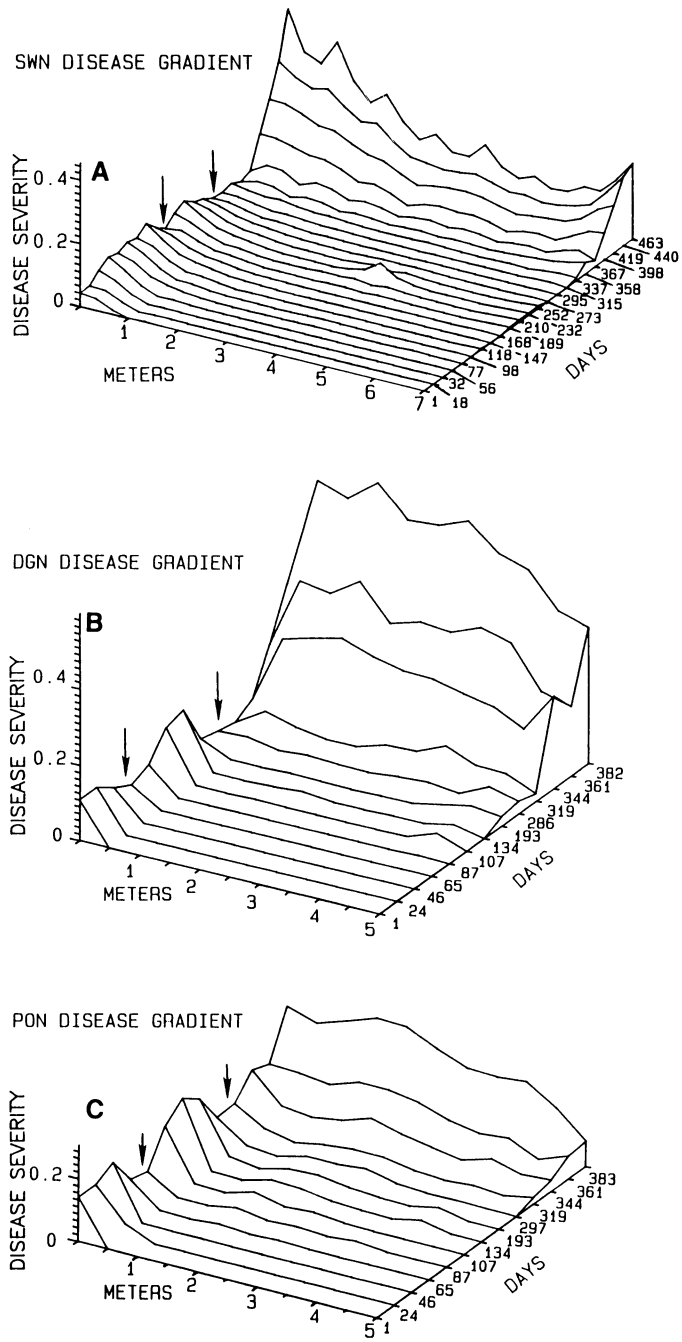

Fig. 5. Nontransformed disease gradients of citrus canker in nurseries over time. Note fluctuations in disease severity near the focus (arrows) in all three nurseries resulting from disease-induced defoliation. DGN = Duncan grapefruit nursery; PON = Pineapple orange nursery; SWN = Swingle rootstock nursery.

by splash alone. Hence, in nurseries splash dispersal and the establishment of secondary foci in close proximity to the original focus seemed to predominate over wind dissemination of inoculum of *X. c. citri*. Directional spread due to wind dissemination was masked quickly by splash dispersal and the early appearance of secondary foci. This effect also is seen in estimates of aggregation of diseased individuals. Aggregation between nursery rows was just as strong or stronger than within rows. Apparently splash dispersal between and within rows is nearly equivalent because of the close lattice spacing of individuals (Fig. 4A and B).

Isopath maps of disease severity provided an excellent means of identifying the spatial location, size, and intensity of secondary foci as well as the coalescence of foci over time (Fig. 3). Most secondary foci seemed to develop within about 3–4 m of the original focus and then spread further from there. Comparison of the intensity of these foci was best accomplished by examination of three-dimensional response surfaces of disease incidence (Fig. 2). The dominance of the primary focus soon was overcome by secondary foci which often developed disease severities greater than the original focus. The fluctuation of these "peaks" of disease severity over time also can be observed. As described previously, decreases in disease severity in more heavily infected individuals was related to disease-induced defoliation (8). Isopath maps have been proposed to study the spatial and temporal rate of movement of isopaths and levels of disease incidence (12). In nurseries infected with CBC, this could be done only until the numerous secondary foci begin to coalesce. The CBC-induced defoliation which caused fluctuations in disease severity thus caused similar fluctuations in the outward progress of isopaths which often regressed inward in some areas. This may be compounded further by the differential rate of outward movement predicted for isopaths of different levels (12).

The fluctuation of disease severity, especially near the focus, also affected disease gradient analysis. These fluctuations occurred twice in each nursery (Fig. 5). The effect of lowering disease incidence values near the focus while the disease expanded outward caused disease gradients to not only flatten but actually to become positive in the case of the grapefruit nursery (Fig. 4D). The seesawing of CBC disease gradient slopes in response to disease-induced defoliation has been described previously for grove epidemics and appears to be inherent to citrus canker epidemics (8).

LITERATURE CITED

1. Agostini, J. P., Graham, J. H., and Timmer, L. W. 1985. Relationship between development of citrus canker and rootstock cultivar for young 'Valencia' orange trees in Misiones, Argentina. Proc. Fla. State Hortic. Soc. 98:19-22.
2. Berger, R. D. 1981. Comparison of the Gompertz and logistic equations to describe plant disease progress. Phytopathology 71:716-719.
3. Civerolo, E. L. 1984. Bacterial canker disease of citrus. J. Rio Grande Val. Hortic. Soc. 37:127-146.
4. Danos, E., Berger, R. D., and Stall, R. E. 1984. Temporal and spatial spread of citrus canker within groves. Phytopathology 74:904-908.
5. Danos, E., Bonazzola, R., Berger, R. D., Stall, R. E., and Miller, J. W. 1981. Progress of citrus canker on some species and combinations in Argentina. Proc. Fla. State Hortic. Soc. 94:15-18.
6. Gabriel, D. W., Kingsley, M. T., Hunter, J. E., and Gottwald, T. R. 1989. Reinstatement of *Xanthomonas citri* (ex. Hasse) and *X. phaseoli* (ex. Smith) to species and reclassification of all *X. campestris* pv. *citri* strains. Int. J. Syst. Bacteriol. 39:14-22.
7. Gottwald, T. R., Civerolo, E. L., Garnsey, S. M., Brlansky, R. H., Graham, J. H., and Gabriel, D. W. 1988. Dynamics and spatial distribution of *Xanthomonas campestris* pv. *citri* group E strains in simulated nursery and new grove situations. Plant Dis. 72:781-787.
8. Gottwald, T. R., McGuire, R. G., and Garran, S. 1988. Asiatic citrus canker: Spatial and temporal spread in simulated new planting situations in Argentina. Phytopathology 78:739-745.
9. Gottwald, T. R., Miller, C., Brlansky, R. H., Gabriel, D. W., and Civerolo, E. L. 1989. Analysis of the spatial distribution of citrus bacterial spot in a Florida citrus nursery. Plant Dis. 73:297-303.
10. Graham, J. H., and Gottwald, T. R. 1988. Citrus canker and citrus bacterial spot in Florida: Research findings—future considerations. Citrus Ind. 69:42-51.
11. Gregory, P. H. 1968. Interpreting plant disease dispersal gradients. Annu. Rev. Phytopathol. 6:189-212.
12. Jeger, M. J. 1984. Models of focus expansion in disease epidemics. Pages 269-288 in: The Movement and Dispersal of Agriculturally Important Biotic Agents: An International Conference on Movement and Dispersal of Biotic Agents, Baton Rouge, LA, October 17-19, 1984.
13. Koizumi, M. 1977. Relation of temperature to the development of citrus canker in the spring. Proc. Int. Soc. Citric. 3:924-928.
14. Koizumi, M. 1981. Citrus canker. Pages 8-12 in: Citrus Diseases in Japan. T. Miyakawa and A. Yamaguchi, eds. Japan Plant Protection Association.
15. Koizumi, M. 1985. Citrus canker: The world situation. Pages 2-7 in: Citrus Canker: An International Perspective. L. W. Timmer, ed. Univ. Fla. Inst. Food Agric. Sci., Gainesville.
16. Madden, L. V. 1980. Quantification of disease progression. Prot. Ecol. 2:159-176.
17. Madden, L. V., Louie, R., Abt, J. J., and Knoke, J. K. 1982. Evaluation of tests for randomness of infected plants. Phytopathology 72:195-198.
18. Peltier, G. L. 1920. Influence of temperature and humidity on the growth of *Pseudomonas citri* and its host plants and on infection and development of the disease. J. Agric. Res. 20:447-506.
19. Peltier, G., and Frederich, W. J. 1924. Further studies on the relative susceptibility to citrus canker of different species and hybrids of the genus *Citrus*, including the wild relatives. J. Agric. Res. 28:227-239.
20. Pennypacker, S. P., Knoble, H. D., Antle, C. E., and Madden, L. V. 1980. A flexible model for studying plant disease progression. Phytopathology 70:232-235.
21. Reedy, B. C. 1984. Incidence of bacterial canker of citrus in relation to weather. Geobios New Rep. 3:39-41.
22. Schoulties, C. L., Civerolo, E. L., Miller, J. W., Stall, R. E., Krass, C. J., Poe, S. R., and DuCharme, E. P. 1987. Citrus canker in Florida. Plant Dis. 71:388-395.
23. Schoulties, C. L., Miller, J. W., Stall, R. E., Civerolo, E. L., and Sasser, M. 1985. A new outbreak of citrus canker in Florida. (Abstr.) Plant Dis. 69:361.
24. Serizawa, S., and Inoue, K. 1975. Studies on citrus canker. III. The influence of wind blowing on infection. Bull. Schizuoka Pref. Citrus Exp. Stn. 11:54-67.
25. Serizawa, S., Inoue, K., and Goto, M. 1969. Studies on citrus canker. I. Dispersal of the citrus canker organism. Bull. Schizouka Pref. Citrus Exp. Stn. 8:81-85.
26. Thal, W. M., Campbell, C. L., and Madden, L. V. 1984. Sensitivity of Weibull model parameter estimates to varieties in simulated disease progression data. Phytopathology 74:1425-1430.
27. Upton, G., and Fingleton, B. 1985. Spatial Data Analysis by Example. John Wiley & Sons, Chichester, England. 410 pp.
28. Vanderplank, J. E. 1963. Plant Diseases: Epidemics and Control. Academic Press, New York. 349 pp.